

RESEARCH

Open Access



Exact solution of cilia induced flow of a Jeffrey fluid in an inclined tube

K. Maqbool¹, S. Shaheen¹ and A. B. Mann^{2*}

*Correspondence:

a_mann27@yahoo.co.uk

² Department of Mathematical Sciences, Federal Urdu University of Arts, Science and Technology, Near Zero Point, G-7/1, Islamabad 44000, Pakistan
Full list of author information is available at the end of the article

Abstract

The present study investigated the cilia induced flow of MHD Jeffrey fluid through an inclined tube. This study is carried out under the assumptions of long wavelength and low Reynolds number approximations. Exact solutions for the velocity profile, pressure rise, pressure gradient, volume flow rate and stream function are obtained. Effects of pertinent physical parameters on the computational results are presented graphically.

Keywords: Cilia, Jeffrey fluid, MHD, Inclined tube

Background

Dutch light microscopist Antoni van Leeuwenhoek discovered cilia in 1675. However, the first comprehensive account of cilia in English language may be credited to Sharpey (1835) who gave the detailed description of ciliary motion in a wide variety of reproductive and respiratory systems of mammals. During the last two decades much progress has been achieved in understanding of ciliary structures. These complex organelles have been examined by a number of experimental techniques. It is noticed that the difference between eukaryotic cilia and flagella is not rigorous. Cilia and flagella are organelles that are primarily used for the transportation of the cell. They propel the cell by flicking back and forth. Cilia motion propels the fluid in which it is moving by its cyclical movements which are asymmetric (Sleigh et al. 1988).

Cilia are short and many per cell and they are reminiscent of hairs whereas flagella are longer and fewer per cell and are reminiscent of a tail. Cilia or flagella shows a variety of beating patterns depending on the surrounding geometry as described in literature (Lindemann and Lesich 2010; Ibacez-Tallon et al. 2003). Cilia beating has been used in regulation (locomotion, ingestion, mixing, etc.). In general, a two-stroke recovery-effective motion is displayed by a single cilium forming the beating pattern. When the cilium is moving towards itself and the neighboring boundary, the recovery (backward) stroke starts, reducing there by the drag on the neighboring fluid in the backward, whereas during the forward stroke, the cilium moves forward into the fluid, dragging the large possible volume of extended fluid. These beating patterns have been considered by various investigators in their works on Cilia motion (Brennen and Winet 1977; Verdugo 1982; Takahashi and Shingyoji 2002; Sanderson and Sleigh 1981; Lardner and Shack 1972).

During the combined motion of cilia, it seems to beat in an organized manner such that upper layer of cilia is deformed in a wave-like manner. This wave is known as metachronal wave, caused by a small angular difference between neighboring cilia, and are just like the waves formed by waving spectators in stadiums. The beat frequency and the metachronal wavelength of cilia are defined as $f = c/2\pi$ and $\lambda = 2\pi/k$ respectively where c is the wave speed and k is the wave number. This collective motion of cilia has been used in many biological studies (Takahashi and Shingyoji 2002; Murakami and Takahashi 1975).

According to the relationship between the forward stroke of the motile cilia and their dynamics, different types of metachronal waves are classified. When the direction of the forward stroke and direction of propagative metachronal wave is same the symplectic beat pattern is formed whereas an antiplectic beat coordination is formed if both directions are opposite to each other (Knight-Jones 1954; Blake 1972).

For the locomotion of mucus by cilia, shear-thinning and elastic effects are assumed. It can diminish the fluid flow opposition at the cilia layer and preserve a semi rigid plane at the superior mucus layer which facilitates the most favorable transport of particles in the respiratory tract. Because of the significance of mucus in an individual's health, many attempts have been made to describe the tracheobronchial mucus transportation (Ross and Corrsin 1974; Blake 1975; Barton and Raynor 1967; Fulford and Blake 1986).

More recently Siddiqui et al. (2014a) examined the hydromagnetic cilia flow of a Newtonian fluid in a symmetric channel using long wavelength approximation. Numerous past experimental observations show that many biological fluids exhibit non-Newtonian characteristics (Siddiqui et al. 2015; Shukla et al. 1980; Srivastava et al. 1983; Brasseur et al. 1987; Narahari and Sreenadh 2010). It is important to note that the cilia induced fluid flow problems play a significant role in non-Newtonian fluid mechanics. Jeffrey fluid model is one of the simplest but the most extensively used models for rheological fluid transports (Hayat et al. 2010; Nadeem and Akbar 2009; Pandey and Tripathi 2010; Kavitha et al. 2012). Viscous properties of human sperm are experimentally found to exhibit Jeffrey behavior (Nadeem and Akram 2010a). Further Jeffrey fluid model has been studied in mechanism of fluid transport specifically in biological systems e.g., urine transport from kidney to bladder through ureter, movement of chyme in the gastrointestinal tract, the movement of spermatozoa in the ducts efferent of the male reproductive tract, ovum in the female fallopian tube, the locomotion of some worms and transport of lymph in the lymphatic vessels (Hayat and Ali 2008). Since the biological fluids are electrically conducted in nature and cilia are present in the airways of lungs which help in protecting from inhaled dust, bacteria and other harmful substances by highly viscous and non-Newtonian mucous (Jeffrey fluid) mainly consisting of water, salt and glycosylated mucin protein (MHD sources) which show the significance of cilia induced flow of MHD Jeffrey fluid in the respiratory tract of humans. The cilia induced flow of Jeffrey fluid in respiratory tract helps in removal of harmful substances trapped in the mucous which are transported along the airways and out of the lungs by the activity of dense mat of microscopic cilia (Smith et al. 2008). By adjusting the various parameters involved in the present study may lead to obtaining results beneficial for removal of tracheobronchial mucous in the respiratory tract. In the present study, mucous is represented by the linearized Jeffrey model valid for small rates of shear and motion is generated due to

constant pressure gradient produced by the cilium tips. Different studies for the Jeffrey fluid model in a symmetric channel under the effect of magnetic field are also available in Hayat and Ali (2008), Kothandapani and Srinivas (2008), Hayat et al. (2008), Nadeem and Akram (2010b), Nallapu and Radhakrishnamacharya (2015) and Saravana et al. (2011). The term cilia used in this paper is restricted to ciliated epithelium.

The aim of this work is to study the transport characteristics through the cilia induced MHD flow of Jeffrey fluid under the low Reynold’s number and long-wavelength approximation in an inclined tube.

Problem formulation

Consider the fluid transport characteristics of an incompressible MHD Jeffrey fluid in an inclined tube under the action of ciliary beat that generates a metachronal wave. The tube having ciliated walls is large in length as compared to radius and a symplectic metachronal wave moves to the right with wave speed c (Siddiqui et al. 2014a, 2015; Smith et al. 2008). The cylindrical coordinate system (R, ϕ, z) is appropriate for the above stated problem. The geometry of the problem under consideration is depicted in Fig. 1.

Cilia are present in the physical model as we have considered the ciliated tube and are hinged near the base at the inner walls of the tube and the fluid motion is generated due to their swing. In existing literature many researchers (Siddiqui et al. 2010, 2015; Akbar et al. 2014, 2016) considered the cilia tips moving in elliptical path which can be represented mathematically in the form

$$R = H = f(z, t) = a + a\epsilon \cos\left(\frac{2\pi}{\lambda}(Z - ct)\right), \tag{1}$$

which is the equation of extensible tube wall, where a is the mean radius of tube, ϵ is the non-dimensional parameter and λ and c are the wavelength and wave speed of metachronal wave respectively. The horizontal position of cilia tips can be written as

$$Z = g(Z, Z_0, t) = Z_0 + a\epsilon\alpha \sin\left(\frac{2\pi}{\lambda}(Z - ct)\right), \tag{2}$$

where Z_0 is the reference position of cilia and α is the eccentricity of ellipse. According to no slip condition the velocity of cilia tips and of fluid adjacent to cilia tips are same, so the Z and R components of velocity are given to be

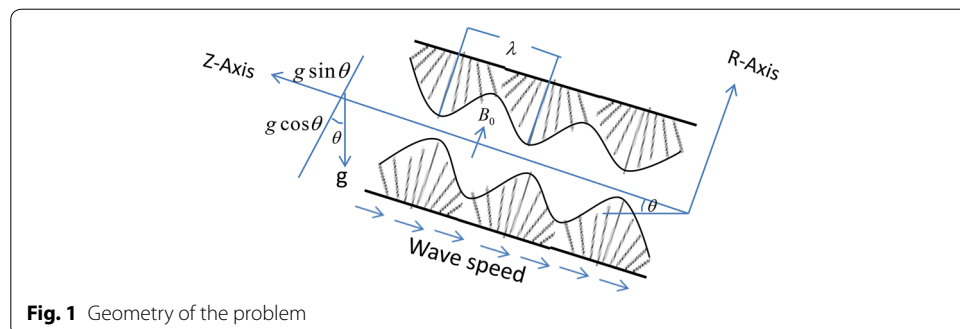


Fig. 1 Geometry of the problem

$$W = \left. \frac{\partial Z}{\partial t} \right|_{Z=Z_0} = \frac{\partial g}{\partial t} + \frac{\partial g}{\partial Z} \frac{\partial Z}{\partial t} = \frac{\partial g}{\partial t} + \frac{\partial g}{\partial Z} W \tag{3}$$

and

$$U = \left. \frac{\partial R}{\partial t} \right|_{Z=Z_0} = \frac{\partial f}{\partial t} + \frac{\partial f}{\partial Z} \frac{\partial Z}{\partial t} = \frac{\partial f}{\partial t} + \frac{\partial f}{\partial Z} W, \tag{4}$$

respectively. Using Eqs. (1–2) in Eqs. (3–4), we arrive at

$$W = \frac{-\left(\frac{2\pi}{\lambda}\right) \left[\epsilon a \alpha c \cos\left(\frac{2\pi}{\lambda}\right) (Z - ct) \right]}{1 - \left(\frac{2\pi}{\lambda}\right) \left[\epsilon a \alpha c \cos\left(\frac{2\pi}{\lambda}\right) (Z - ct) \right]} \tag{5}$$

and

$$U = \frac{\left(\frac{2\pi}{\lambda}\right) \left[a \epsilon \alpha c \sin\left(\frac{2\pi}{\lambda}\right) (Z - ct) \right]}{1 - \left(\frac{2\pi}{\lambda}\right) \left[\epsilon a \alpha c \cos\left(\frac{2\pi}{\lambda}\right) (Z - ct) \right]}, \tag{6}$$

where U and W are the velocity components in axial and radial directions, respectively. A uniform magnetic field of strength B_0 is applied in the direction perpendicular to the cilia induced axial flow. The transformations relating the wave frame (r, z) , moving with velocity c , to the fixed frame (R, Z) are given by

$$z = Z - ct, \quad r = R, \quad w = W - c, \quad u = U \quad \text{and} \quad p(z, r) = P(Z, R, T), \tag{7}$$

where P is the pressure in fixed frame.

The mass and momentum equations which govern the unsteady MHD flow of an incompressible Jeffrey fluid in an inclined tube can be written as (Hayat et al. 2008; Nadeem and Akram 2010b; Nallapu and Radhakrishnamacharya 2015)

$$\nabla \cdot \mathbf{V} = 0, \tag{8}$$

where

$$\mathbf{V} = [u(r, z), 0, w(r, z)] \tag{9}$$

and

$$\rho \frac{d\mathbf{V}}{dt} = \text{div}\mathbf{T} + \mathbf{J} \times \mathbf{B} + \rho \mathbf{g}, \tag{10}$$

where

$$\mathbf{T} = -p\mathbf{I} + \mathbf{S}, \tag{11}$$

$$\mathbf{S} = \frac{\mu}{1 + \lambda_1} \left(\mathbf{A}_1 + \lambda_2 \frac{d\mathbf{A}_1}{dt} \right) \tag{12}$$

and

$$\begin{aligned} \nabla \cdot \mathbf{B} = 0, \quad \nabla \times \mathbf{B} = \mu_m \mathbf{J}, \quad \nabla \times \mathbf{E} = -\frac{\partial \mathbf{B}}{\partial t}, \\ \mathbf{J} = \sigma [\mathbf{E} + \mathbf{V} \times \mathbf{B}] \end{aligned} \tag{13}$$

In above equations ρ is the fluid density, σ is the electrical conductivity, \mathbf{g} is the acceleration force, \mathbf{T} is the Cauchy stress tensor, \mathbf{I} is the identity tensor, \mathbf{S} is the extra stress tensor, \mathbf{A}_1 is the first Rivlin Ericksen tensor, $\lambda_i (i = 1, 2)$ are the fluid parameters, \mathbf{J} is the current density, μ_m is the magnetic permeability and \mathbf{E} is the total electric field, \mathbf{B} is the total magnetic field so that $\mathbf{B} = \mathbf{B}_0 + \mathbf{b}$, \mathbf{b} is the induced magnetic field and is neglected compared with applied magnetic field \mathbf{B}_0 which is in the transverse direction of the flow. In the present analysis, it is assumed that no applied and polarization voltages exist i.e. $\mathbf{E} = 0$. This then corresponds to the case where no energy is added or extracted from the fluid by the electric field.

In the light of above assumptions and due to small magnetic Reynold's number the magnetohydrodynamic force in Eq. (10) is given by

$$\mathbf{J} \times \mathbf{B} = -\sigma B_0^2 (w + c) \hat{e}_z \tag{14}$$

The following dimensionless variables are used to make the quantities dimensionless.

$$\begin{aligned} z^* = \frac{z}{\lambda}, \quad r^* = \frac{r}{a}, \quad u^* = \frac{u}{\beta c}, \quad w^* = \frac{w}{c}, \quad h^* = \frac{H}{a}, \quad p^* = \frac{a\beta}{c\mu} p, \quad t^* = \frac{ct}{\lambda}, \\ \beta = \frac{a}{\lambda}, \quad S_{ij}^* = \frac{a}{\mu c} S_{ij}, \quad M = \sqrt{\frac{\sigma}{\mu}} a B_0, \quad Re = \frac{\rho c a}{\mu}, \quad \text{and} \quad Fr = \frac{c^2}{g a}. \end{aligned} \tag{15}$$

In view of (15), the non-dimensional radial and axial momentum equations become

$$Re\beta^3 \left[\frac{\partial u}{\partial t} + u \frac{\partial u}{\partial r} + w \frac{\partial u}{\partial z} \right] = -\frac{\partial p}{\partial r} + \beta \frac{1}{r} \frac{\partial}{\partial r} (r S_{rr}) - \beta \frac{S_{\theta\theta}}{r} + \beta^2 \frac{\partial S_{zr}}{\partial z} - \beta \frac{Re}{Fr} \cos \theta, \tag{16}$$

$$\beta \left[\frac{\partial w}{\partial t} + u \frac{\partial w}{\partial r} + w \frac{\partial w}{\partial z} \right] = -\frac{\partial p}{\partial z} + \frac{1}{r} \frac{\partial}{\partial r} (r S_{rz}) + \beta \frac{\partial S_{zz}}{\partial z} - M^2 (w + 1) + \frac{Re}{Fr} \sin \theta, \tag{17}$$

where

$$S_{rz} = \frac{\mu}{1 + \lambda_1} \left(\frac{\partial w}{\partial r} + \beta \frac{\partial u}{\partial z} \right) + \lambda_2 \left(\beta u \frac{\partial^2 w}{\partial r^2} + u \beta^3 \frac{\partial^2 u}{\partial r \partial z} + \beta w \frac{\partial^2 w}{\partial r \partial z} + \beta^3 w \frac{\partial^2 u}{\partial z^2} \right). \tag{18}$$

The appropriate boundary conditions will take the form

$$u = \frac{2\pi \epsilon \sin(2\pi z)}{1 - 2\pi \epsilon \alpha \beta \cos(2\pi z)} \tag{19}$$

and

$$w = \frac{-2\pi \epsilon \alpha \beta \cos(2\pi z)}{1 - 2\pi \epsilon \alpha \beta \cos(2\pi z)} - 1, \quad \text{at } r = h = 1 + \epsilon \cos(2\pi z). \tag{20}$$

Further, the centerline symmetry requires

$$\frac{\partial w}{\partial r} = 0, \quad \text{at } r = 0. \tag{21}$$

Since the flows in small diameter tubules are inertia free therefore the analysis in the present study can be approximated under the long wavelength or small Reynold’s number approximations i.e., $(\beta \rightarrow 0, Re \ll 1)$ (Shapiro et al. 1969). So the governing equations with boundary conditions (16–21) under the long wavelength approximation can be simplified to

$$\frac{\partial^2 w}{\partial r^2} + \frac{1}{r} \frac{\partial w}{\partial r} - M^2(1 + \lambda_1)w = (1 + \lambda_1) \left(\frac{\partial p}{\partial z} - \frac{Re}{Fr} \sin \theta + M^2 \right), \tag{22}$$

$$\frac{\partial p}{\partial r} = 0, \tag{23}$$

$$\frac{\partial w}{\partial r} = 0, \quad \text{at } r = 0 \quad \text{and} \quad w = w(h) = -1 - 2\pi\epsilon\alpha\beta \cos(2\pi z) \tag{24}$$

and

$$u = u(h) = 2\pi\epsilon \sin(2\pi z) + \beta(2\pi\epsilon)^2\alpha \sin(2\pi z) \cos(2\pi z). \tag{25}$$

Solution of the problem

From Eq. (23), it is evident that $p \neq p(r)$ and hence p is the function of z alone therefore Eq. (22) becomes

$$\gamma^2 \frac{\partial^2 w}{\partial r^2} + \gamma \frac{\partial w}{\partial r} - M^2\gamma^2(1 + \lambda_1)w = (1 + \lambda_1)\gamma^2 \left(\frac{dp}{dz} - \frac{Re}{Fr} \sin \theta + M^2 \right), \tag{26}$$

with boundary conditions

$$u = u(h) = 2\pi\epsilon \sin(2\pi z) + \beta(2\pi\epsilon)^2\alpha \sin(2\pi z) \cos(2\pi z), \tag{27}$$

and

$$\frac{\partial w}{\partial r} = 0, \quad \text{at } r = 0 \quad \text{and} \quad w = w(h) = -1 - 2\pi\epsilon\alpha\beta \cos(2\pi z). \tag{28}$$

Solving the non-homogeneous Bessel’s Eq. (26) with the help of boundary conditions (27, 28), we arrive at

$$w = w(h) \frac{I_0(\sqrt{1 + \lambda_1}Mr)}{I_0(\sqrt{1 + \lambda_1}Mh)} + \left(1 + \frac{1}{M^2} \frac{dp}{dz} - \frac{1}{M^2} \frac{Re}{Fr} \sin \theta \right) \left(\frac{I_0(\sqrt{1 + \lambda_1}Mr)}{I_0(\sqrt{1 + \lambda_1}Mh)} - 1 \right), \tag{29}$$

where I_0 is the modified Bessel’s function of first kind and order zero.

Integrating Eq. (8)

$$\int_0^h \left[\frac{1}{r} \frac{\partial(ru)}{\partial r} + \frac{\partial w}{\partial z} \right] r dr = 0, \tag{30}$$

we yield

$$hu(h) + \frac{1}{2} \frac{\partial q}{\partial z} - h \frac{\partial h}{\partial z} w(h) = 0, \tag{31}$$

where $q = 2 \int_0^h wrdr$. Equation (31) can be written as

$$\frac{\partial q}{\partial z} = 2h \left(\frac{\partial h}{\partial z} w(h) - u(h) \right) = 0. \tag{32}$$

Again integrating Eq. (29) over the cross section of tube, the pressure gradient can be written in terms of volume flow rate as

$$\begin{aligned} \frac{dp}{dz} = & \frac{q\sqrt{1 + \lambda_1}M^3I_0(\sqrt{1 + \lambda_1}Mh) - 2M^2hw(h)I_1(\sqrt{1 + \lambda_1}Mh)}{2hI_1(\sqrt{1 + \lambda_1}Mh) - h^2M\sqrt{1 + \lambda_1}I_0(\sqrt{1 + \lambda_1}Mh)} \\ & + M^2 \frac{Re}{Fr} \sin \theta - M^2, \end{aligned} \tag{33}$$

where I_1 is the modified Bessel's function of first kind and order one. Substituting the value of $\frac{dp}{dz}$ in Eq. (29), we get

$$\begin{aligned} w = & w(h) \frac{I_0(\sqrt{1 + \lambda_1}Mr)}{I_0(\sqrt{1 + \lambda_1}Mh)} + \left(\frac{I_0(\sqrt{1 + \lambda_1}Mr)}{I_0(\sqrt{1 + \lambda_1}Mh)} - 1 \right) \\ & \times \left\{ 1 + \left(\frac{q\sqrt{1 + \lambda_1}MI_0(\sqrt{1 + \lambda_1}Mh) - 2hw(h)I_1(\sqrt{1 + \lambda_1}Mh)}{2hI_1(\sqrt{1 + \lambda_1}Mh) - h^2M\sqrt{1 + \lambda_1}I_0(\sqrt{1 + \lambda_1}Mh)} \right. \right. \\ & \left. \left. + M^2 \frac{Re}{Fr} \sin \theta - M^2 \right) - \frac{1}{M^2} \frac{Re}{Fr} \sin \theta \right\}. \end{aligned} \tag{34}$$

In order to find the pressure rise, we shall integrate Eq. (33) with respect to z from 0 to h which results in

$$\Delta p = qM^3\sqrt{1 + \lambda_1}I_1^* - 2M^2I_2^* + M^2 \frac{Re}{Fr} \sin \theta - M^2, \tag{35}$$

where

$$I_1^* = \int_0^1 \frac{I_0(\sqrt{1 + \lambda_1}Mh)}{2hI_1(\sqrt{1 + \lambda_1}Mh) - h^2M\sqrt{1 + \lambda_1}I_0(\sqrt{1 + \lambda_1}Mh)} dz, \tag{36}$$

and

$$I_2^* = \int_0^1 \frac{hw(h)I_1(\sqrt{1 + \lambda_1}Mh)}{2hI_1(\sqrt{1 + \lambda_1}Mh) - h^2M\sqrt{1 + \lambda_1}I_0(\sqrt{1 + \lambda_1}Mh)} dz. \tag{37}$$

The integrals appearing in (36–37) are solved by using the software “**Mathematica**”. The relation between q and dimensionless volume flow rate Q is given by

$$Q = 2 \int_0^h WRdR = 2 \int_0^h (w + 1)rdr = q + h^2. \tag{38}$$

The mean volume flow rate for the time period $T = \frac{t}{c}$ is

$$\bar{Q} = \frac{1}{T} \int_0^T Q dt^* = q + 1 + 0.5\epsilon^2. \tag{39}$$

Now using the relation

$$\Delta p = (\bar{Q} - 1 - 0.5\epsilon^2)M^3\sqrt{1 + \lambda}I_1^* - 2M^2I_2^* + M^2\frac{Re}{Fr} \sin \theta - M^2, \tag{40}$$

Equation (40) can be written as

$$\bar{Q} = \frac{\Delta p + M^2 - M^2\frac{Re}{Fr} \sin \theta + 2M^2I_2^*}{2I_1^*M^3\sqrt{1 + \lambda}} + 1. \tag{41}$$

The radial velocity for the case of Jeffrey fluid can be evaluated from Eq. (30) as

$$\begin{aligned} u = & -\frac{\partial w(h)}{\partial z} \frac{I_1(\sqrt{1 + \lambda_1}Mr)}{I_0(\sqrt{1 + \lambda_1}Mh)} + w(h) \frac{I_1(\sqrt{1 + \lambda_1}Mr)I_1(\sqrt{1 + \lambda_1}Mh)}{I_0^2(\sqrt{1 + \lambda_1}Mh)} \frac{\partial h}{\partial z} \\ & + \left(\frac{1}{M^2} \frac{dp}{dz} + 1 - \frac{1}{M^2} \frac{Re}{Fr} \sin \theta \right) \left(\frac{I_1(\sqrt{1 + \lambda_1}Mr)I_1(\sqrt{1 + \lambda_1}Mh)}{I_0^2(\sqrt{1 + \lambda_1}Mh)} \frac{\partial h}{\partial z} \right) \\ & - \frac{1}{M^2} \frac{d^2p}{dz^2} \left(\frac{I_1(\sqrt{1 + \lambda_1}Mr)}{M\sqrt{1 + \lambda_1}I_0(\sqrt{1 + \lambda_1}Mh)} - \frac{r}{2} \right). \end{aligned} \tag{42}$$

Similarly, the stream function can be evaluated by the help of velocity profile and is given by

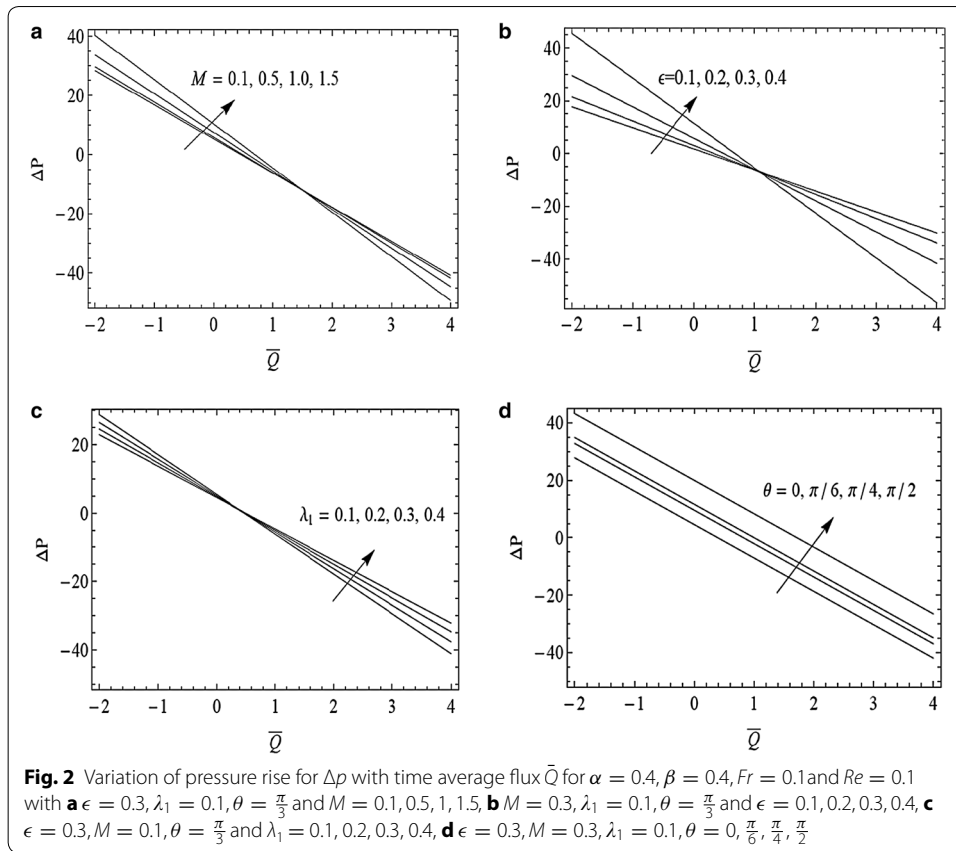
$$\begin{aligned} \psi = & rw(h) \frac{I_1(\sqrt{1 + \lambda_1}Mr)}{I_0(\sqrt{1 + \lambda_1}Mh)} + \left(\frac{1}{M^2} \frac{dp}{dz} + 1 - \frac{1}{M^2} \frac{Re}{Fr} \sin \theta \right) \\ & \times \left(\frac{rI_1(\sqrt{1 + \lambda_1}Mr)}{M\sqrt{1 + \lambda_1}I_0(\sqrt{1 + \lambda_1}Mh)} - \frac{r^2}{2} \right). \end{aligned} \tag{43}$$

The results presented above correspond to the results of Siddiqui et al. (2014b) when both λ_1 and inclination angle θ approach zero.

Numerical results and discussion

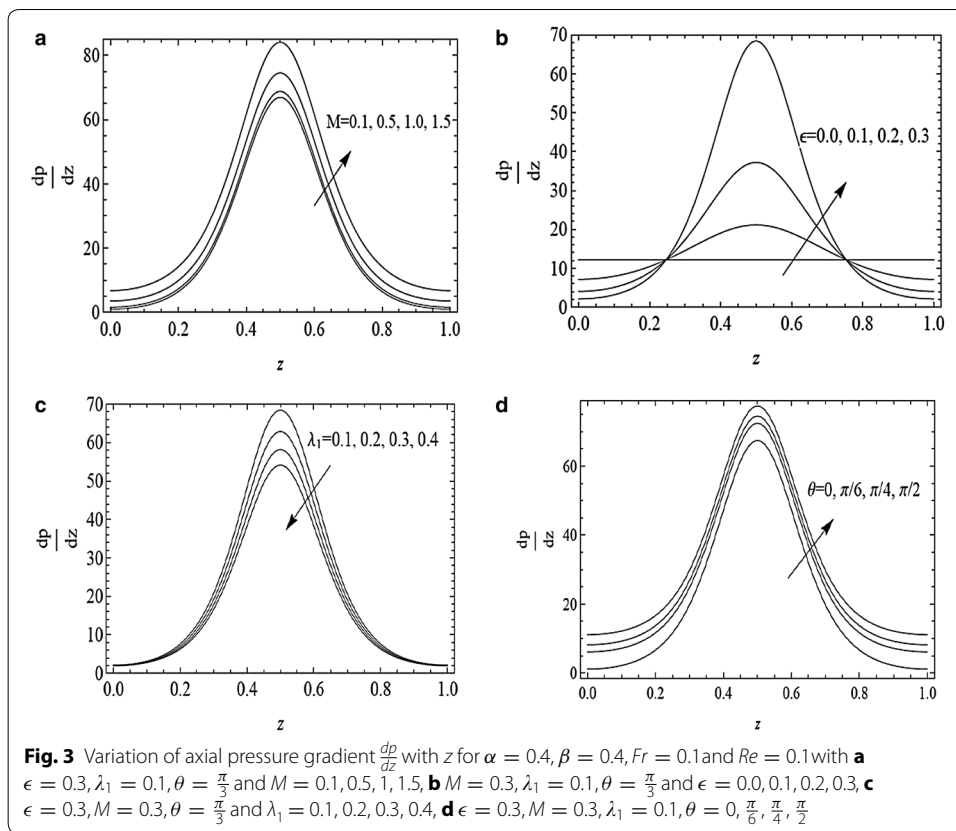
In this section, the graphical illustrations of the results obtained in the last sections are presented to show the effects of various parameters of interest. In particular the effect of distinct parameters for the pressure rise, axial velocity, axial pressure gradient and stream function are observed.

The variation of pressure rise Δp with time average flux \bar{Q} , for different values of Hartmann number M , cilia length ϵ , Jeffrey parameter λ_1 , and angle of inclination θ , are examined in Fig. 2a–d. It is noted that pressure rise increases with an increase in



Hartmann number M in the region ($\bar{Q} < 1, \Delta p > 0$). However a converse trend is noted in region ($\bar{Q} > 1, \Delta p < 0$). Figure 2b shows an increase in pressure rise with increase in ϵ in the interval $-2 \leq \bar{Q} \leq 1$. However, it decreases by increasing ϵ for $\bar{Q} > 1$. Figure 2c indicates a decrease in pressure rise by increasing Jeffrey parameter λ_1 in the interval $-2 \leq \bar{Q} \leq 0.5$ while its behavior is reversed when $0.5 \leq \bar{Q} \leq 4$. Figure 2d indicates that pressure rise increases by increasing angle of inclination θ in the whole interval $-2 \leq \bar{Q} \leq 4$.

The variation of axial pressure gradient $\frac{dp}{dz}$ with z for different values of M, ϵ, λ_1 and θ is depicted in Fig. 3a–d. It is observed that pressure gradient is small in the region $0 \leq z \leq 0.28$ and $0.78 \leq z \leq 1$ and fluid can flow easily without applying a large pressure gradient but a large amount of pressure gradient is required to maintain the same flux in the region $0.28 < z < 0.78$. Also by increasing the Hartmann number M , the amplitude of $\frac{dp}{dz}$ increases. Fig. 3b reveals that the amplitude of the pressure gradient increases with an increase of cilia parameter ϵ in the region $0.28 \leq z \leq 0.78$. From Fig. 3c it is noticed that by increasing the Jeffrey parameter λ_1 , the amplitude of the pressure gradient in the centre of the tube decreases whereas no pressure gradient is required to maintain the flow at the ends of the tube. Figure 3d shows that increase in angle of inclination increases the amplitude of the pressure gradient i.e., inclined tube requires a large



amount of pressure gradient to flow in the region $[0.28, 0.78]$ as compared to the inlet and outlet of the tube.

In Fig. 4a–d axial velocity behavior is examined for different values of prominent parameters. Figure 4a shows that by increasing the magnetic parameter, the axial velocity decreases near the axis of tube because the Lorentz’s force resists the fluid to flow in the centre of the tube due to magnetic field whereas fluid is at rest on the lateral surface of the tube. Figure 4b shows that increase in cilia length decreases the magnitude of the axial velocity at the centre of the tube while in the vicinity of the walls the axial velocity also decreases but in the opposite direction. From Fig. 4c, one can notice that magnitude of the axial velocity decreases in the centre of the tube by increasing the Jeffrey parameter i.e., the fluid becomes thick which retards the fluid flow in reverse direction. Figure 4d shows that by increasing the angle of inclination, magnitude of the axial velocity decreases at the centre of the tube but reverse trend is observed near the boundary walls, i.e., the inclined tube resists the flow in the reverse direction.

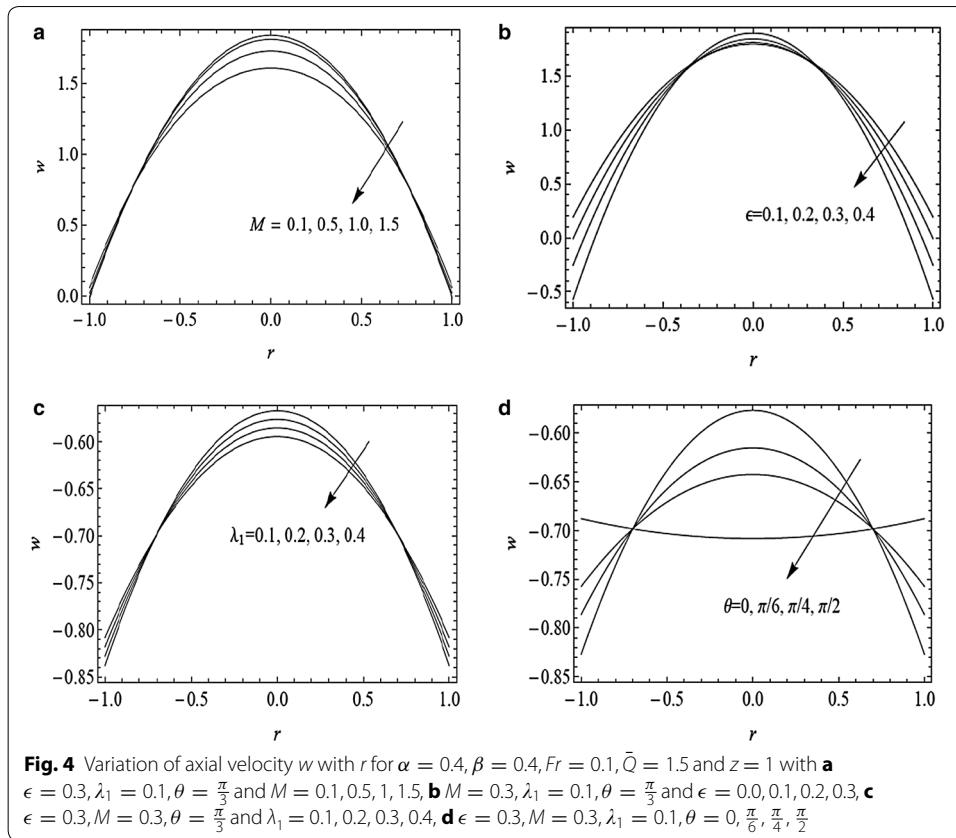
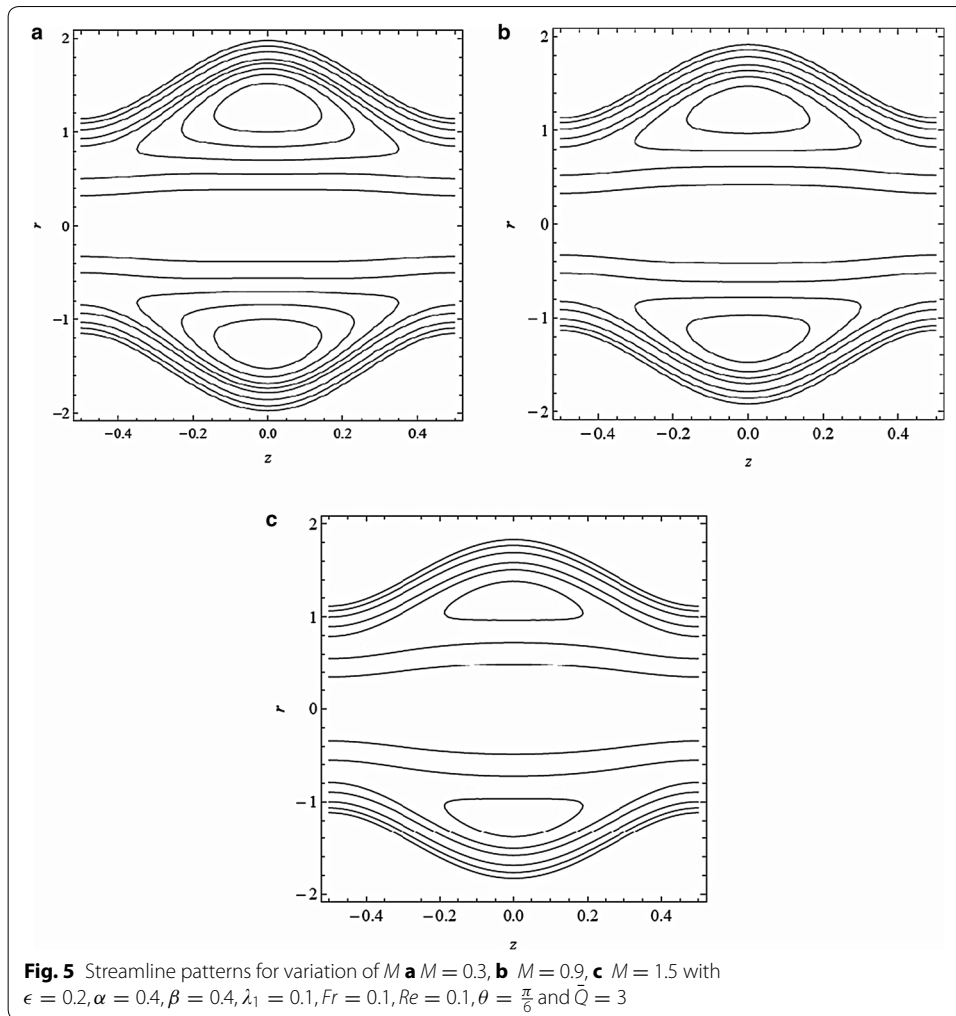
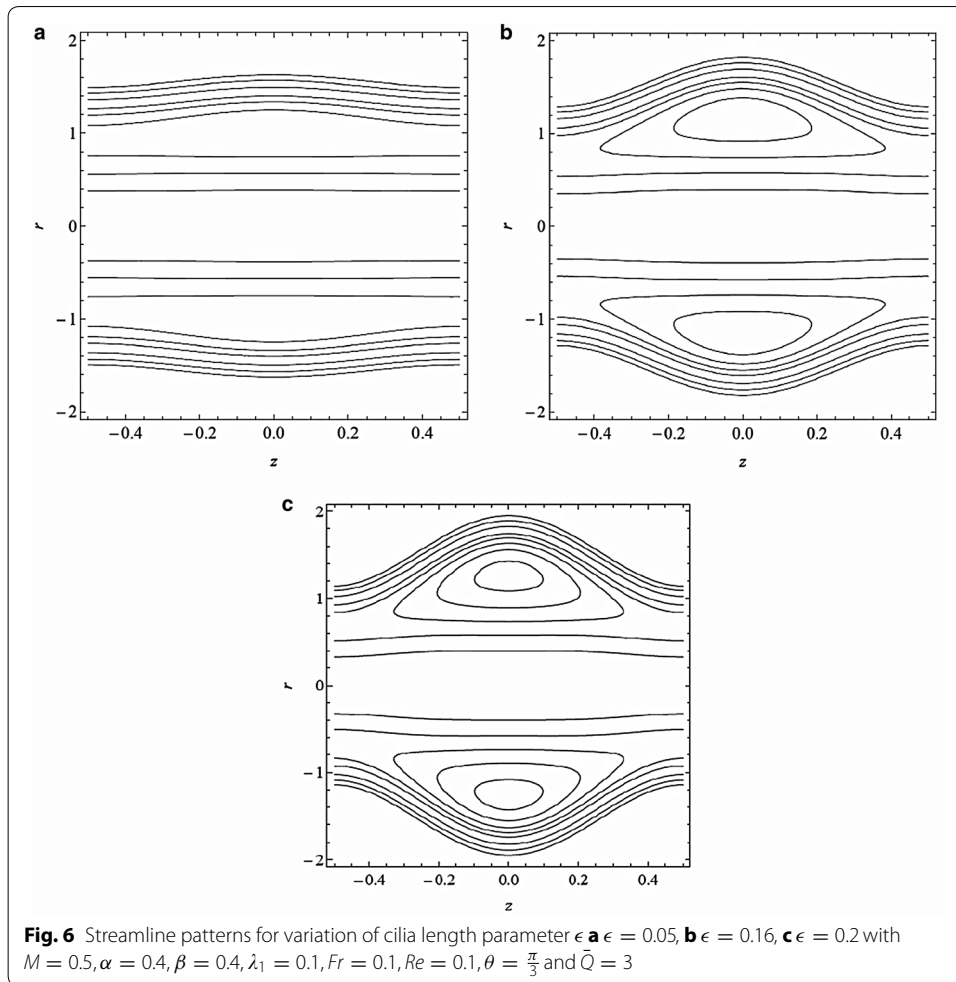


Figure 5a–c show the graphs of streamlines for different values of Hartmann parameter M . It is observed that the size and circulation of the trapped bolus decrease with an increase in the value of M . It is further noted that the trapped bolus disappears for $M = 1.5$. This might be due to decelerating effect of magnetic force on the flow velocity. Figure 6a–c highlight that the size and circulation of the trapped boluses increase by increasing the cilia length parameter ϵ which indicates that circulation formed by the ciliary movement is dominant by increasing the cilia length. Figure 7a–c depict that the size of the bolus decreases with increase in the angle of inclination θ which shows that this parameter has significant effect on the viscosity of the the fluid.

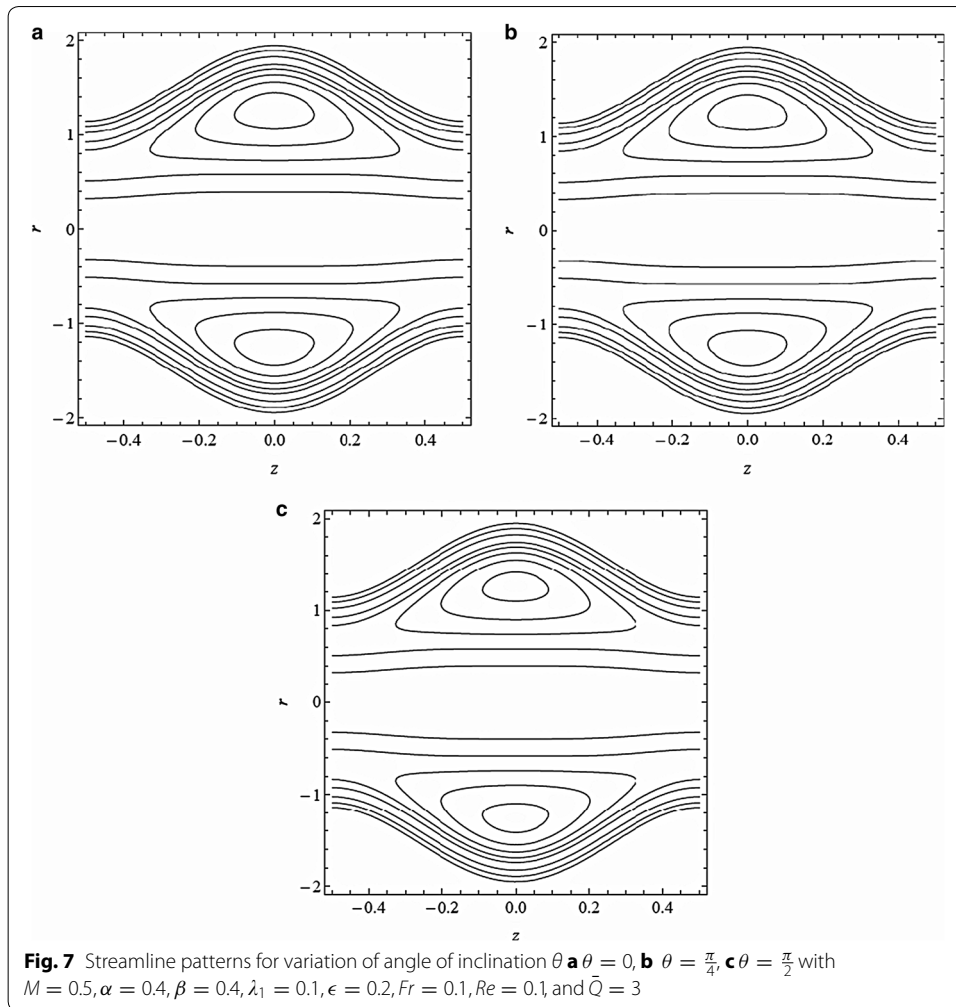


Conclusions

In this paper we have presented a theoretical approach to study ciliary motion of Jeffrey fluid in an inclined tube under the effect of magnetic field. The fluid flow is induced by the metachronal wave formed at cilia tip. The tube symmetry is produced by considering the metachronal wave on the cilia tip adjacent to fluid layer. We have adopted the long wavelength and low Reynolds number approximations that simplifies the problem. Cilia motion in Newtonian and non-Newtonian fluids is a current topic of interest. Different studies exit in literature in which the cilia induced flow in different geometries and



stresses are discussed (Siddiqui et al. 2010, 2014a, b 2015; Akbar et al. 2014, 2016). The exact analytical results obtained by Siddiqui et al. (2014b) can be captured as a limiting case (by taking θ and $\lambda_1 \rightarrow 0$) and are found to be in good agreement with the results of Siddiqui et al. (2014b). The effects of cilia length parameter ϵ , Hartmann number M , Jeffrey parameter λ_1 and angle of inclination θ on pressure rise Δp , pressure gradient $\frac{dp}{dz}$, axial velocity w and stream function ψ are investigated. It is observed that the amplitude of the pressure gradient increases with the increase in angle of inclination, Hartmann number and cilia length whereas the amplitude of $\frac{dp}{dz}$ decreases by increasing the Jeffrey



parameter in the centre of the tube. Further the velocity profiles decrease by increasing the Hartmann number but reverse effect is observed by increasing the Jeffrey parameter.

List of symbols

U, W : velocity components in the fixed frame; u, w : velocity components in the wave frame; R, Z : cylindrical polar coordinates in fixed frame; r, z : cylindrical polar coordinates in wave frame; P : pressure in fixed frame; p : pressure in wave frame; t : time; f, g : parametric representations of elliptical path; a : average radius of the tube; c : speed of metachronal wave; g : acceleration due to gravity; J : current density; B : total magnetic field; M : Hartmann number; Re : Reynolds number; Fr : Froude number; Q : volume flow rate; \bar{Q} : average volume flow rate; $\frac{dp}{dz}$: pressure gradient; Δp : pressure rise; α : eccentricity of the elliptical path; ρ : fluid density; μ : viscosity; λ_1, λ_2 : Jeffrey fluid parameters; θ : angle of inclination; ψ : stream function; ϵ : cilia length; λ : wavelength of metachronal wave; β : ratio of a and λ ; σ : electrical conductivity.

Authors' contributions

This work is the product of intellectual effort of all the authors. KM and ABM designed and suggested the problem. KM, SS and ABM solved the problem jointly. KM and SS wrote the paper. KM and ABM critically reviewed the final draft. All authors read and approved the final manuscript.

Author details

¹ Department of Mathematics and Statistics, International Islamic University, Islamabad 44000, Pakistan. ² Department of Mathematical Sciences, Federal Urdu University of Arts, Science and Technology, Near Zero Point, G-7/1, Islamabad 44000, Pakistan.

Acknowledgements

Authors are grateful to their institutions for providing necessary research and technical facilities. We are grateful to the reviewers for their painstaking review, constructive comments and detailed suggestions for improving the quality of paper.

Competing interests

The authors declare that they have no competing interests.

Received: 12 April 2016 Accepted: 8 August 2016

Published online: 22 August 2016

References

- Akbar NS, Khan ZH, Nadeem S (2014) Metachronal beating of cilia under influence of Hartmann layer and heat transfer. *Eur Phys J Plus* 129:176
- Akbar NS, Khan ZH, Nadeem S (2016) Influence of magnetic field and slip on Jeffrey fluid in a ciliated symmetric channel with metachronal wave pattern. *J Appl Fluid Mech* 9(2):565–572
- Barton C, Raynor S (1967) Analytical investigation of cilia-induced mucous flow. *Bull Math Biophys* 29(3):419–428
- Blake JR (1972) A model for the micro-structure in ciliated organisms. *J Fluid Mech* 55:1–23
- Blake JR (1975) On the movement of mucus in the lungs. *J Biomech* 8:179–190
- Brasseur JG, Corrsin S, Lu Nan Q (1987) The influence of a peripheral layer of different viscosity on peristaltic pumping with Newtonian fluids. *J Fluid Mech* 174:495–519
- Brennen C, Winet H (1977) Fluid mechanics of propulsion by cilia and flagella. *Ann Rev Fluid Mech* 9:339–398
- Fulford GR, Blake JR (1986) Muco-ciliary transport in the lung. *J Theor* 121(4):381–402
- Hayat T, Ali N (2008) Peristaltic motion of a Jeffrey fluid under the effect of magnetic field in a tube. *Commun Nonlinear Sci Numer Simul* 13(7):1343–1352
- Hayat T, Ahmad N, Ali N (2008) Effects of an endoscope and magnetic field on the peristalsis involving Jeffrey fluid. *Commun Nonlinear Sci Numer Simul* 13(8):1581–1591
- Hayat T, Ali N, Asghar S (2010) An analysis of peristaltic transport for flow of a Jeffrey fluid. *Acta Mech* 193(1):101–112
- Ibacez-Tallon I, Heintz N, Omran H (2003) To beat or not to beat: roles of cilia in development and disease. *Hum Mol Genet* 12:R27
- Kavitha A, Reddy RH, Srinivas ANS, Sreenadh S, Saravana R (2012) Peristaltic transport of a Jeffrey fluid in a porous channel with suction and injection. *Int J Mech Mater Eng* 7(2):152–157
- Knight-Jones EW (1954) Relations between metachronism and the direction of ciliary beat in metazoa. *Q J Microsc Sci* 95:503–521
- Kothandapani M, Srinivas S (2008) Peristaltic transport of a Jeffrey fluid under the effect of magnetic field in an asymmetric channel. *Int J Non-linear Mech* 43(9):915–924
- Lardner TJ, Shack WJ (1972) Cilia transport. *Bull Math Biol* 34(16):325–335
- Lindemann CB, Lesich KA (2010) Flagellar and ciliary beating: the proven and the possible. *J Cell Sci* 123:519–528
- Murakami A, Takahashi K (1975) Correlation of electrical and mechanical responses in nervous control of cilia. *Nature* 257:48–49
- Nadeem S, Akbar NS (2009) Peristaltic flow of a Jeffrey fluid with variable viscosity in an asymmetric channel. *Z Naturforsch A* 64a:713–722
- Nadeem S, Akram S (2010a) Peristaltic flow of a Jeffrey fluid in a rectangular duct. *Nonlinear Anal Real World Appl* 11(5):4238–4247
- Nadeem S, Akram S (2010b) Slip effects on the peristaltic flow of a Jeffrey fluid in an asymmetric channel under the effect of induced magnetic field. *Int J Numer Methods Fluids* 63(3):374–394
- Narahari M, Sreenadh S (2010) Peristaltic transport of a Bingham fluid in contact with a Newtonian fluid. *Int J Appl Math Mech* 6(11):41–54
- Nallapu S, Radhakrishnamacharya G (2015) Jeffrey fluid flow through a narrow tubes in the presence of a magnetic field. *Procedia Eng* 127:185–192
- Pandey SK, Tripathi D (2010) Unsteady model of transport of Jeffrey fluid by Peristalsis. *Int J Biomath* 3(4):473–491
- Ross SM, Corrsin S (1974) Results of an analytical model of mucociliary pumping. *J Appl Physiol* 37(3):333–340
- Sanderson MJ, Sleight MA (1981) Ciliary activity of cultured rabbit tracheal epithelium: beat pattern and metachrony. *J Cell Sci* 47:331–347
- Saravana R, Sreenadh S, Venkataramana S, Reddy RH, Kavitha A (2011) Influence of slip conditions, wall properties and heat transfer on MHD peristaltic transport of a Jeffrey fluid in a nonuniform porous channel. *Int J Innov Technol Creat Eng* 1(11):10–24
- Shapiro AH, Jaffrin MY, Weinberg SL (1969) Peristaltic pumping with long wavelength at low Reynolds number. *J Fluid Mech* 37:799–825
- Shukla JB, Parihar RS, Rao BRP, Gupta SP (1980) Effects of peripheral layer viscosity on peristaltic transport of a bio fluid. *J Fluid Mech* 97:225–237
- Siddiqui AM, Haroon T, Rani M, Ansari AR (2010) An analysis of the flow of a power law fluid due to ciliary motion in an infinite channel. *J Biorheol* 24(2):56–69
- Siddiqui AM, Farooq AA, Rana MA (2014a) Hydromagnetic flow of Newtonian fluid due to ciliary motion in a channel. *Magnetohydrodynamics* 50(3):109–122

- Siddiqui AM, Farooq AA, Rana MA (2014b) Study of MHD effects on the cilia-induced flow of a Newtonian fluid through a cylindrical tube. *Magnetohydrodynamics* 50(4):249–261
- Siddiqui AM, Farooq AA, Rana MA (2015) An investigation of non-Newtonian fluid flow due to metachronal beating of cilia in a tube. *Int J Biomath* 8(2):1550016-1-1550016-23
- Sleigh MA, Blake JR, Liron N (1988) The propulsion of mucus by cilia. *Am Rev Respir Dis* 137:726–741
- Smith DJ, Gaffney EA, Blake JR (2008) Modelling mucociliary clearance. *Respir Physiol Neurobiol* 163:178–188
- Srivastava LM, Srivastava VP, Sinha SN (1983) Peristaltic transport of a physiological fluid part—I: flow in non-uniform geometry. *Biorheology* 20:153–166
- Takahashi K, Shingyoji C (2002) Control of eukaryotic flagella and cilia. *Zool Sci* 19:1393–1394
- Verdugo P (1982) Introduction: mucociliary function in mammalian epithelia. *Cell Motil Suppl* 2:1–5

Submit your manuscript to a SpringerOpen[®] journal and benefit from:

- ▶ Convenient online submission
- ▶ Rigorous peer review
- ▶ Immediate publication on acceptance
- ▶ Open access: articles freely available online
- ▶ High visibility within the field
- ▶ Retaining the copyright to your article

Submit your next manuscript at ▶ springeropen.com
